CUO molecule and the Ar atoms of the model cages. We are examining these interactions carefully, especially in light of the recent report of the new stable argon molecule HArF.[13]

The potential energy surfaces (PES) along the bending coordinate are quite complicated for both the $^1\Sigma^+$ ground state and the $^3\Phi$ excited state of linear CUO. Although CUO is isoelectronic to UO_2^{2+}, the U–O and U–C interactions are much more localized in CUO than are the symmetry-equivalent U–O interactions in UO_2^{2+}. As such, the bending PES for both states are quite shallow, which leads to very small predicted bending frequencies ($< 75\ cm^{-1}$) in both the ground and excited state. Upon bending, the $^1\Sigma^+$ and $^3\Phi$ states correlate to $^1A'$ and $^3A'+^3A''$ states under C_s symmetry, and interaction of the $^1A'$ with both the $^3A'$ and $^3A''$ states will be allowed by spin–orbit (SO) coupling. We are currently undertaking higher level calculations on CUO, including SO effects, to better chart the relative energetics of this fascinating molecule.

Received: July 17, 2000 [Z15463]

[1] Recent examples: a) M. F. Zhou, L. Andrews, *J. Chem. Phys.* **1999**, *110*, 10370 (Fe + CO); b) M. F. Zhou, L. Andrews, *J. Am. Chem. Soc.* **1999**, *121*, 9171 (Rh + CO); c) M. F. Zhou, L. Andrews, *J. Phys. Chem. A* **1999**, *103*, 7785 (Nb, Ta + CO).

[2] U + N_2: a) R. D. Hunt, J. T. Yustein, L. Andrews, *J. Chem. Phys.* **1993**, *98*, 6070; b) G. P. Kushto, P. F. Souter, L. Andrews, *J. Chem. Phys.* **1998**, *108*, 7121.

[3] U + CO: M. F. Zhou, L. Andrews, J. Li, B. E. Bursten, *J. Am. Chem. Soc.* **1999**, *121*, 9712.

[4] Th + CO: M. F. Zhou, L. Andrews, J. Li, B. E. Bursten, *J. Am. Chem. Soc.* **1999**, *121*, 12188.

[5] U, Th + CO_2: L. Andrews, M. F. Zhou, B. Liang, J. Li, B. E. Bursten, *J. Am. Chem. Soc.* **2000**, in press.

[6] P. Pyykkö, J. Li, N. Runeberg, *J. Phys. Chem.* **1994**, *98*, 4809.

[7] ADF 2.3, Theoretical Chemistry, Vrije Universiteit, Amsterdam. Relevant references: a) E. J. Baerends, D. E. Ellis, P. Ros, *Chem. Phys.* **1973**, *2*, 42; b) G. te Velde, E. J. Baerends, *J. Comput. Phys.* **1992**, *99*, 94; c) C. Fonseca Guerra, O. Visser, J. G. Snijders, G. te Velde, E. J. Baerends in *Methods and Techniques for Computational Chemistry* (Eds: E. Clementi, G. Corongiu), STEF, Cagliari, **1995**, p. 305.

[8] T. R. Burkholder, L. Andrews, *J. Chem. Phys.* **1991**, *95*, 8697.

[9] R. D. Hunt, L. Andrews, *J. Chem. Phys.* **1993**, *98*, 3690.

[10] M. F. Zhou, L. Andrews, *J. Chem. Phys.* **1999**, *111*, 11044.

[11] M. E. Jacox, *Chem. Phys.* **1994**, *189*, 149.

[12] Strictly speaking, spin is no longer a good quantum number because of spin–orbit coupling and it is not rigorously correct to speak of a "triplet" state. Under spin–orbit coupling, the 4σ HOMO and 1ϕ LUMO transform into the $7e_{1/2}$ and $1e_{5/2} + 1e_{7/2}$ spinors, respectively, with the $1e_{7/2}$ spinor greatly destabilized (0.65 eV) relative to the $1e_{5/2}$ spinor. Thus, under spin–orbit coupling, the ground state of the isolated molecule corresponds to the $(7e_{1/2})^2$ configuration, and the first excited state corresponds to the $(7e_{1/2})^1(1e_{5/2})^1$ configuration. Because spin-polarization energy is an important factor in actinide complexes, these two states will be dominantly singlet and triplet in character, respectively, and we will use these descriptors for clarity.

[13] L. Khriachtchev, M. Pettersson, N. Runeberg, J. Lundell, M. Räsänen, *Nature* **2000**, *406*, 874.

Visualization of Single Multivalent Receptor–Ligand Complexes by Transmission Electron Microscopy**

Jason E. Gestwicki, Laura E. Strong, and Laura L. Kiessling*

Multivalent ligands have the capacity to interact simultaneously with multiple receptors. The binding of a divalent ligand, for example, can bring two receptors together.[1, 2] Many natural and synthetic ligands are not divalent, however, but rather contain many possible receptor binding sites.[3] The complexation of such multivalent ligands with multiple receptors may be important for their biological activities.[4, 5] Unfortunately, whether multiple receptors bind to a multivalent ligand and how many associate in a complex often can only be inferred. The difficulties associated with investigating such molecular details are exacerbated by the lack of tools available to characterize these binding events.

Previous efforts to study multivalent receptor–ligand complexes have used light scattering,[6] fluorescence resonance energy transfer,[7–9] capillary electrophoresis,[10] or analytical ultracentrifugation. Transmission electron microscopy (TEM) methods are complementary to these indirect measurements as they allow direct visualization of complexes.[11–13] Another advantage of TEM experiments is that since single molecules or complexes can be viewed the amount of material needed is typically less than that required for other techniques. Prior applications of electron microscopy to examine multiple receptors interacting with a ligand have focused on large complexes that can be imaged directly.[14, 15] Many important receptor–ligand complexes, however, are too small or of insufficient density to be directly imaged in this way. Here we report a strategy that extends the range of receptor–ligand complexes that can be imaged by TEM.

We reasoned that a method that increased the contrast of receptors would allow visualization of receptors bound to a given ligand and facilitate the characterization of individual small receptor–ligand complexes. Our solution employs colloidal gold particles as labels to monitor the receptor position in the presence of a ligand. Because of its density, colloidal gold allows high-contrast imaging by electron microscopy. This approach is routinely taken in immunohistochemical applications, in which cellular proteins are located by colloidal gold particles attached to antibodies. Proteins other than antibodies can be attached to colloidal gold, and streptavidin-conjugated gold particles of different sizes are readily available. Such particles are used commonly because

[*] Prof. L. L. Kiessling, J. E. Gestwicki, L. E. Strong
Departments of Chemistry and Biochemistry
University of Wisconsin-Madison
Madison, WI 53706 (USA)
Fax: (+1) 608-262-3453
E-mail: kiessling@chem.wisc.edu

[**] The authors thank Colleen Lavin (UW Madison, Microscopy Resource) and Kim Dickson for experimental support. This work was supported in part by the NIH (GM 55984). J.E.G. acknowledges the NIH Biotechnology Training Grant for support (T32GM08349). L.E.S. was supported by an NIH predoctoral fellowship (GM 18750).

  1433-7851/00/3924-4567 $ 17.50+.50/0

of the high affinity of the streptavidin for biotin ($K_d = 10^{-15}$ M). By attaching a single biotin group to a target receptor the number of receptors complexed to a multivalent ligand can be visualized through detection of the streptavidin-conjugated gold particles. This approach provides a general method for visualizing a wide range of complexes formed between receptors and multivalent ligands.

To illustrate the utility of TEM for characterizing multivalent binding events we explored the binding of the lectin concanavalin A (Con A) to a series of multivalent ligands that vary in average length and valency. Con A is a tetrameric mannose-binding plant lectin that has been used as a model for the study of multivalent interactions.[16–18] We have synthesized mannose-substituted ligands by ring-opening metathesis polymerization (ROMP)[19] that are potent inhibitors of Con A function.[20–22] Ligands of different lengths and valencies have been generated by this strategy; these have unique properties relative to their monovalent counterparts.[23, 24] Significantly, we found that as the average ligand valency increased from 1 to 50, the activities of the mannose-substituted materials increased dramatically ($10^2 - 10^5$-fold) in assays with Con A.[21, 22, 25] Thus, ligand valency is an important determinant of ligand potency in this system. The influence of ligand valency may stem from the number of receptors that can assemble on a particular ligand. TEM was used to characterize complexes between Con A and synthetic mannose ligands **1**–**4** to determine whether this mode of complexation occurs (Figure 1).

The complexation experiments employed Con A tetramers that were labeled with biotin using conditions that favored attachment of a low number of biotin residues (namely, 1–2 copies per tetramer). The resulting tetramers were allowed to associate with a ligand of interest (**1**–**4**) in solution. Complexes of biotinylated Con A and ligand were then treated with an excess of streptavidin-bound 10-nm gold particles. These solutions were spread on grids and viewed by TEM. In some experiments samples were treated with 2% phosphotungstic acid (pH 7.0 for 30 seconds) to enhance the contrast. Images of random fields (Figure 2) were acquired for each treatment and analyzed for formation of Con A complexes. Gold particles within 25 nm or less of each other were considered to be part of a complexes. This distance was based on the modeled length of the synthetic, multivalent ligands[21] and the structure of tetrameric Con A determined by X-ray crystallographic analysis.[26] The number of gold particles employed was chosen to minimize their coincidental adjacent placement while maximizing the relevant data that could be obtained from each experiment.

The number of gold particles incorporated into complexes was determined to assess the ability of **1**–**4** to bind multiple copies of Con A (Figure 3). Only the multivalent ligands **2**–**4** were able to interact simultaneously with multiple Con A tetramers. Importantly, the number of Con A tetramers bound depended on the valency of the ligand. In the presence of compound **2** complexes that contain two copies of Con A predominate (referred to as "dimers" in Figure 3). With compounds **3** and **4** complexes possessing three Con A tetramers (referred to as "trimers" in Figure 3) were observed in addition to those with two. When **4** is the multivalent ligand

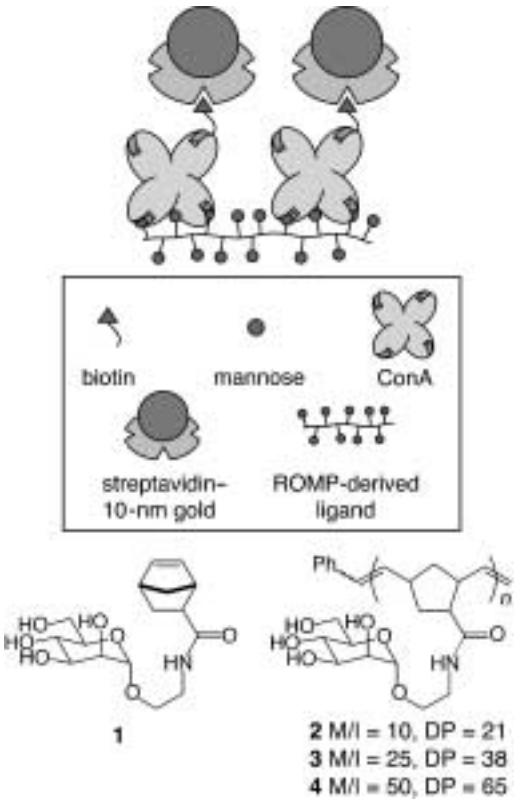

Figure 1. General strategy for the visualization of multivalent ligand complexes with receptors using transmission electron microscopy (TEM). In this example, biotinylated Con A tetramers are added to multivalent mannose-bearing ligands synthesized by ROMP. After complexation, streptavidin-conjugated gold particles are added. The resulting clusters are visualized by TEM as described in the text. The synthesis of ligands **1**–**4** is described elsewhere.[20] The value *n* is determined by the monomer to initiator ratio (M/I) used in the synthesis. The average polymer length (degree of polymerization, DP) was determined by comparison of the integration of the phenyl proton signal in the ^{1}H NMR spectrum with that of the signal corresponding to the backbone protons.

the higher order complex (trimer) is favored. As ligand valency increases, therefore, the average number of Con A receptors bound to each ligand also increases. These results suggest that the previously observed increases in activities for ligands of higher valency may be derived from their abilities to bind and/or cluster multiple copies of Con A.[21]

Multivalent receptor–ligand interactions are an integral component of many biological systems. The ability of a multivalent ligand to cluster receptors may be an important determinant of its biological activity.[27, 28] We have shown that TEM can be used to illuminate the features of individual multivalent complexes and obtain information on populations of these complexes. Our data reveal that this method is effective even for relatively weak receptor–ligand interactions (Con A binds mannose with a $K_d \approx 1$ mM). Higher affinity interactions, therefore, are expected to yield similar or better results. Additionally, the TEM experiments disclosed here can be used to relate the number of receptors associated with a ligand to its functional affinity and biological activity, a critical step in elucidating the mechanism(s) by which multivalent ligands function.

  1433-7851/00/3924-4568 $ 17.50+.50/0

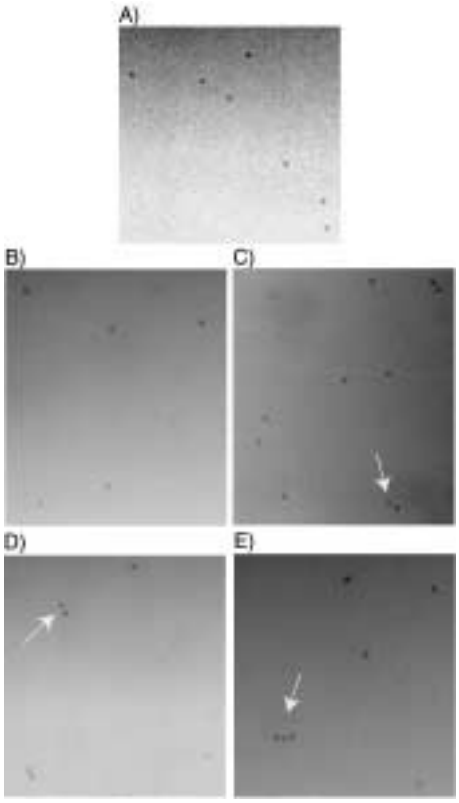

Figure 2. Images of sample fields from electron microscopy experiments using streptavidin-conjugated gold particles of biotinylated Con A: A) without ligand; B) with **1**; C) with **2**; D) with **3**; E) with **4**. Fields are representative segments of those collected for three experiments. Approximately 10–20 fields (80–150 gold particles) were collected during each independent experiment and a total of 250–650 gold particles were counted for each treatment. The arrows point to dimers in (C) and (D) and a trimer in (E). Magnification is 12500×.

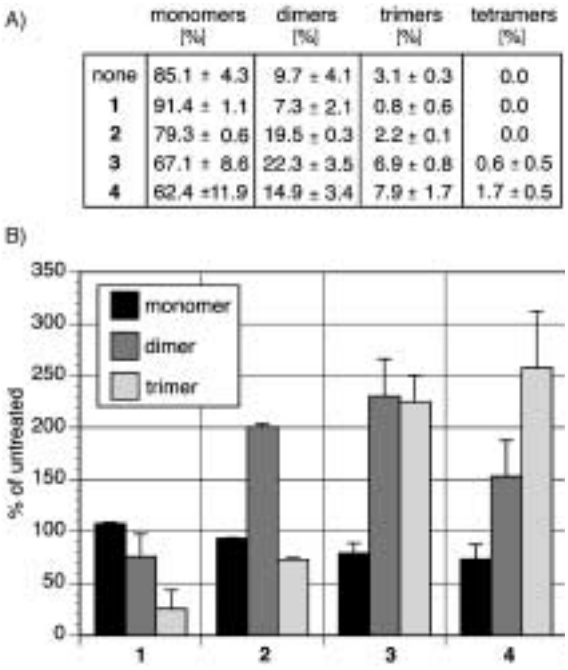

Figure 3. The number of biotinylated Con A tetramers bound by the ligand depends on the valency of the ligand partner. A) The number of gold particles incorporated into complexes (complexes are termed monomers, dimers, trimers, and tetramers as described in the text) are shown for each treatment as a percentage of the total number of gold particles counted. Dimers were defined as two gold particles within 25 nm. Trimers and tetramers were defined as three and four gold particles within this distance, respectively. Three experiments were performed on separate days using freshly prepared grids. On each day, 80–150 gold particles were counted from approximately 10–20 images of random fields for each treatment. The percentage of each complex type (monomer–tetramer) was determined on each day and the final reported percentages are averages of the three experiments. The errors represent single standard deviations. B) Graphical representation of data. Results are expressed as a percentage of untreated (biotinylated Con A and streptavidin-bound 10-nm gold particles alone). The number of monomers decreases with increasing ligand valency, while the number of clusters (dimers and trimers) increases. Error bars represent single standard deviations.

Experimental Section

Biotinylation reactions: These were carried out in 0.1M sodium borate at pH 8.8 for 12 h at room temperature using a Con A concentration of 1 mg mL^{-1} and a final biotinylating reagent concentration ranging from 0 to 500 μg mL^{-1} in a final volume of 1 mL. Each reaction was quenched with a 1M aqueous solution of NH_4Cl. The biotinylating reagent was sulfosuccinimidyl-6-(biotinamido) hexanoate (EZ-link Sulfo-NHS-LC-Biotin, Pierce, Rockford, IL). Biotinylated Con A was dialyzed extensively against 10 mM 2-[4-(2-hydroxyethyl)-1-piperazinyl]ethanesulfonic acid (HEPES) pH 7.0 at 4 °C to remove excess biotin. The protein concentration after dialysis was determined by a Bradford assay using bovine serum albumin (BSA) as a standard. Molar ratios of biotin to Con A were determined using 2-(4′-hydroxyazobenzene)-benzoic acid (HABA, Pierce) according to the manufacturers specifications. The Con A used in the subsequent electron microscopy experiment had a biotin to Con A tetramer ratio of 1.9:1, and was derived from a reaction with a starting biotinylating reagent concentration of 5 μg mL^{-1}.

Electron microscopy: Biotinylated Con A (2.3 μM tetramers) and ligand (0.75 μM mannose) in phosphate-buffered saline (PBS) pH 7.2 were mixed. These solutions (5 μL) were incubated for 15 min at room temperature before streptavidin-bound 10-nm gold particles (3.0 μM) were added. The molar ratio of ligand:Con A:streptavidin in the optimized assay was 1:3:4. No insoluble biotinylated Con A complexes were observed. The streptavidin concentration was determined by the bicinchoninic acid (BCA) method using BSA as a standard. TEM was performed using Formvar-treated grids on a LEO Omega 912 EFTEM. Images were collected on a ProScan Slow Scan CCD camera and processed in Adobe Photoshop 5.0. Images were analyzed for complex formation manually, using the 10-nm gold particles as a convenient internal size standard. Occasionally, large aggregates of gold were observed in the preparations, these particles were discounted from the analysis and could be removed by centrifugation prior to sample preparation.

Received: July 26, 2000 [Z15535]

[1] O. Livnah, E. A. Stura, D. L. Johnson, S. A. Middelton, L. S. Mulcahy, N. C. Wrighton, W. J. Dower, L. K. Jolliffe, I. A. Wilson, *Science* **1996**, *273*, 464–470.
[2] O. Livnah, E. A. Stura, S. A. Middleton, D. L. Johnson, L. K. Joliffe, I. A. Wilson, *Science* **1999**, *283*, 987–990.
[3] M. Mammen, S.-K. Choi, G. M. Whitesides, *Angew. Chem.* **1998**, *110*, 2908–2953; *Angew. Chem. Int. Ed.* **1998**, *37*, 2755–2794.
[4] R. N. Germain, *Curr. Biol.* **1997**, *7*, R640–644.
[5] H. Metzger, *J. Immunol.* **1992**, *149*, 1477–1487.
[6] A. V. Timoshenko, I. V. Gorudko, S. N. Cherenkevich, H.-J. Gabius, *FEBS Letters* **1999**, *449*, 75–78.
[7] K. L. Carraway III, J. G. Koland, R. A. Cerione, *J. Biol. Chem.* **1989**, *264*, 8699–8707.
[8] J. Matko, M. Edidin, *Methods Enzymol.* **1997**, *278*, 444–462.
[9] S. D. Burke, Q. Zhao, M. C. Schuster, L. L. Kiessling, *J. Am. Chem. Soc.* **2000**, *122*, 4518–4519.
[10] K. Shimura, K. Kasai, *Electrophoresis* **1998**, *19*, 397–402.
[11] K. T. Hiriyanna, J. Varkey, M. Beer, R. M. Benbow, *J. Cell Biol.* **1988**, *107*, 33–44.

  1433-7851/00/3924-4569 $ 17.50+.50/0

[12] S. R. Simmons, R. M. Albrecht, *Scanning Microsc. Suppl.* **1989**, *3*, 27 – 34.
[13] R. C. Mucic, J. J. Storhoff, C. A. Mirkin, R. L. Letsinger, *J. Am. Chem. Soc.* **1998**, *120*, 12674 – 12675.
[14] K. Matsubara, S. Ebina, *Adv. Biophys.* **1997**, *34*, 253 – 262.
[15] D. Gupta, L. Bhattacharyya, J. Fant, F. Macaluso, S. Sabesan, C. F. Brewer, *Biochemistry* **1994**, *33*, 7495 – 7504.
[16] R. S. Singh, A. K. Tiwary, J. F. Kennedy, *Crit. Rev. Biotechnol.* **1999**, *19*, 145 – 178.
[17] W. I. Weis, K. Drickamer, *Annu. Rev. Biochem.* **1996**, *65*, 441 – 473.
[18] S. M. Dimick, S. C. Powell, S. A. McMahon, D. N. Moothoo, J. H. Naismith, E. J. Toone, *J. Am. Chem. Soc.* **1999**, *121*, 10286 – 10296.
[19] L. L. Kiessling, L. E. Strong, *Top. Organomet. Chem.* **1998**, *1*, 199 – 231.
[20] L. E. Strong, L. L. Kiessling, *J. Am. Chem. Soc.* **1999**, *121*, 6193 – 6196.
[21] M. Kanai, K. H. Mortell, L. L. Kiessling, *J. Am. Chem. Soc.* **1997**, *119*, 9931 – 9932.
[22] D. A. Mann, M. Kanai, D. J. Maly, L. L. Kiessling, *J. Am. Chem. Soc.* **1998**, *120*, 10575 – 10582.
[23] E. J. Gordon, W. J. Sanders, L. L. Kiessling, *Nature* **1998**, *392*, 30 – 31.
[24] W. J. Sanders, E. J. Gordon, O. Dwir, P. J. Beck, R. Alon, L. L. Kiessling, *J. Biol. Chem.* **1999**, *274*, 5271 – 5278.
[25] K. H. Mortell, M. Gingras, L. L. Kiessling, *J. Am. Chem. Soc.* **1994**, *116*, 12053 – 12054.
[26] S. Parkin, B. Rupp, H. Hope, *Acta Crystallogr. Sect. D* **1996**, *52*, 1161 – 1168.
[27] C.-H. Heldin, *Cell* **1995**, *80*, 213 – 223.
[28] J. D. Klemm, S. L. Schreiber, G. R. Crabtree, *Annu. Rev. Immunol.* **1998**, *16*, 569 – 592.

A Remarkable, Stable Radical – Molecule Complex: $HO_2 \cdot CF_3C(O)OH$

Joseph S. Francisco

The hydrogen bond is of considerable interest in understanding the structure and energetics in a wide range of chemical systems.[1–3] Many studies have examined hydrogen bonding in neutral molecule – molecule and ion – molecule complexes,[4] but few have focused on radical – molecule complexes. A vigorous research effort is just beginning to examine fundamental questions of hydrogen bonding in open-shell complexes. Molecular complexes are generally weakly bound[5, 6] and hence relatively short-lived. Such complexes are reported to play key roles in the Earth's atmosphere.[7] Strongly bound complexes of atmospheric species suggest long atmospheric lifetimes, and this leads to the possibility of their being transported to remote regions of the atmosphere, where their concentration profiles are not expected to be large. The atmospheric oxidation of alternative fluoro- and chlorofluorocarbons, such as HFC-134a, HCFC-123, and HCFC-124, is a major atmospheric source of trifluoroacetic acid (TFA).[8, 9] Because of the increased use and production of alternative chlorofluorocarbons, TFA concentrations are projected to increase.[10] Trifluoroacetic acid is chemically and biologically stable and highly resistant to photochemical breakdown. To date, little evidence is available for the degradation of TFA; consequently, little is known about the consequences of trifluoroacetic acid for atmospheric chemistry. Here we report on density functional calculations that suggest the existence of a complex between trifluoroacetic acid and $HO_2^{\bullet}$ radicals. The structural and energetic data of the complex suggest novel bonding and stability that have important ramifications for the atmospheric role of trifluoroacetic acid.

Unrestricted density functional calculations with Becke's three parameters and Lee – Yang – Parr functionals (UB3LYP)[11, 12] with the 6-311++G(3df,3pd) basis set were carried out. The fully optimized geometries with minimum energies were confirmed to be stable minima by vibrational frequency analysis.[13] Only the global minimum energy structure is reported in this study. The structure of $HO_2 \cdot CF_3C(O)OH$ (Figure 1) is characterized by two hydrogen

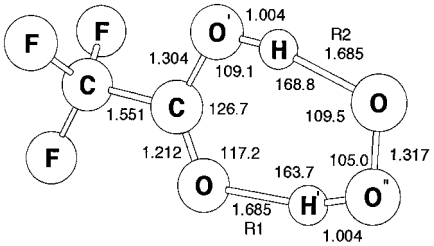

Figure 1. Structure and geometry of $HO_2 \cdot CF_3C(O)OH$.

bonds, labeled R1 and R2. The hydrogen bond between the hydrogen atom of the hydroperoxyl radical and the carbonyl oxygen atom of the trifluoroacetic acid has a length of 1.685 Å, as does that between the hydroxyl hydrogen atom of trifluoroacetic acid and the terminal oxygen atom of the hydroperoxyl radical. These bonds are both significantly shorter than the typical hydrogen-bond lengths in the water dimer (ca. 1.95 Å) and in the well-studied formic acid/H_2O complex (1.786 Å). Unlike weakly bound complexes, in which the structures of the components are virtually unaffected by hydrogen bonding, there is a significant degree of structural perturbation of the geometry of the two components as a result of the bonding in the $HO_2 \cdot CF_3C(O)OH$ complex. The C–O′ bond in trifluoroacetic acid is shortened by 0.032 Å (i.e., 2.4%), and the O–H bond is lengthened by 0.037 Å (i.e., 3.8%). The O–H bond length in the $HO_2^{\bullet}$ radical in the complex is lengthened by 0.029 Å (i.e., 3.0%) relative to isolated $HO_2^{\bullet}$. These structural changes indicate strong interactions in the $HO_2 - CF_3C(O)OH$ complex.

The bonding energies at various levels of theory are presented in Table 1. At the highest level of theory, the binding energy D_o and well depth D_e of $HO_2 \cdot CF_3C(O)OH$ are 15.1 and 17.1 kcal mol^{-1}, respectively. Considering that the water dimer[14–16] has a well depth of about 4.8 kcal mol^{-1}, this is tremendous. Typically, hydrogen bonds have energies of 2 – 7 kcal mol^{-1} and are thought to involve essentially linear arrangements of donor and proton acceptors.[1, 16, 17] In this case, each component acts as a hydrogen donor and acceptor,

[*] Prof. Dr. J. S. Francisco
Department of Chemistry and Department of Earth and Atmospheric Sciences
Purdue University
West Lafayette, IN 47907 – 1393 (USA)
Fax: (+1) 765-494-0239
E-mail: jfrancis@purdue.edu

  1433-7851/00/3924-4570 $ 17.50+.50/0